Analyst

Accepted Manuscript

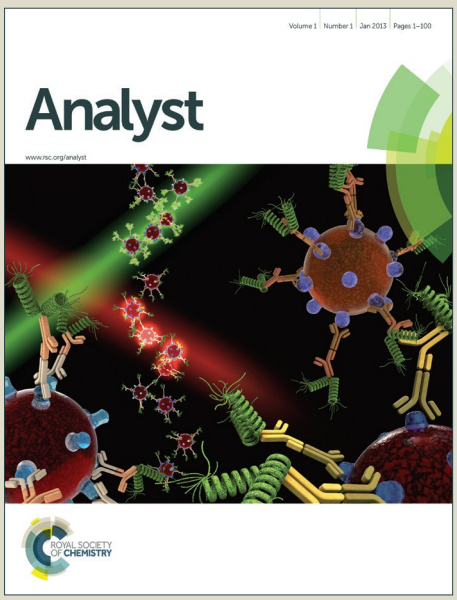

ROYAL SOCIETY OF CHEMISTRY

www.rsc.org/analyst

Analyst

ARTICLE

Electrochemical sensing of etoposide by using carbon quantum dots modified glassy carbon electrode

Received 00th January 20xx,
Accepted 00th January 20xx

DOI: 10.1039/x0xx00000x

www.rsc.org/

Hoai Viet Nguyen[a,b], Lukas Richtera[a,b] Amitava Moulick[a,b], Kledi Xhaxhiu[c], Jiri Kudr[a,b], Natalia Cernei[a,b], Hana Polanska[b,d], Zbynek Heger[a,b], Michal Masarik[b,d], Pavel Kopel[a,b], Marie Stiborova[e], Tomas Eckschlager[f], Vojtech Adam[a,b], Rene Kizek[a,b*]

In this study, it is demonstrated the enhancement of electrochemical signals of etoposide (ETO) by modifying glassy carbon electrode (GCE) with carbon quantum dots (CQDs) measured by differential pulse voltammetry (DPV). In comparison with bare GCE, modified GCE exhibited higher sensitivity of ETO electrochemical detection. The lowest limit of detection is observed as 5 nM ETO. Furthermore, scanning electron microscopy (SEM), fluorescence microscopy (FM), and electrochemical impedance spectroscopy (EIS) were employed for further studying of working electrode surface after modifying with CQDs. Finally, GCE modified with CQDs under optimized conditions was used to analyse real samples of ETO in prostate cancer cell line PC3. After different times of incubation (1, 3, 6, 9, 12, 18 and 24 h), these samples were prepared prior to electrochemical detection by GCE modified with CQDs. High performance liquid chromatography with electrochemical detection method was employed to verify results from GCE modified with CQDs.

1. Introduction

Carbon based materials are well known for their potential applications in various fields.[1-6] Range of carbon based materials in different forms includes inter alia, carbon nanotubes (CNT), graphene, graphene oxide, and carbon quantum dots (CQDs).[7-11] CQDs have significantly attracted the research community due to their fascinating properties including size, and inexpensive nature.[12] In addition, they have widely achieved progress because of their good solubility, strong luminescence, and more often they are also referred as carbon nanolights.[12, 13] The promising biological properties of CQDs, including low toxicity and biocompatibility, confer them with significant potential applications in biosensing, bioimaging, optronics and catalysis and drug delivery.[12, 14, 15]

Etoposide (ETO) or VP-16 is an anticancer drug, which showed high potential to be deliverable by various nanomaterials including abovementioned carbon ones.[16] ETO is a semi-synthetic derivative of podophyllotoxin, which was used for the treatment of a variety of malignancies, including small-cell lung cancer and other solid tumours.[17-19] The mechanism of action of ETO is still unknown but it is a cell-cycle, phase specific drug that appears to act either by forming free radicals or causing DNA breaks by an interaction with DNA-topoisomerase II.[20-26] Therefore, the appearance as well as changing amount of ETO in the biological samples plays an important role in cancer therapy. Numerous qualitative and quantitative methods have been used for determination of ETO such as high performance liquid chromatography (HPLC),[27-32] liquid chromatography-mass spectrometry,[33, 34] micellar electrokinetic chromatography,[35] and electrochemical detection.[20, 36, 37] Electrochemical measurements show promising alternative to classical methods due to their relatively low operational cost and good miniaturization potential enabling rapid and sensitive detection with especially faster and more accurate analysis.

In this study, a novel electrochemical sensing system based on CQDs modified glassy carbon electrode (GCE) has been developed for the sensitive determination of ETO. Surface modification is an effective way to tune the morphological properties of materials for wide range of specific applications. Number of approaches has been made for functionalizing the surface of CQDs by changing the surface chemistry or interactions.[38-41] Most of CQDs are rich in oxygen-containing groups, which allow the possibility to modify the surface layer to increase the activity of CQDs. The CQDs used in this study were functionalized by terminal –COOH groups using polyvinylpyrrolidone (PVP) showing excellent photo-reversibility and high stability.[42, 43]

[a] Department of Chemistry and Biochemistry, Mendel University in Brno, Zemedelska 1, CZ-613 00 Brno, Czech Republic, European Union
[b] Central European Institute of Technology, Brno University of Technology, Technicka 3058/10, CZ-616 00 Brno, Czech Republic, European Union
[c] Department of Chemistry, Faculty of Natural Sciences, University of Tirana, Blv. Zog I, No.2/1, 1001, Tirana, Albania
[d] Department of Pathological Physiology, Faculty of Medicine, Masaryk University, Komenskeho namesti 2, Brno CZ-662 43, Czech Republic, European Union
[e] Department of Biochemistry, Faculty of Science, Charles University, Albertov 2030, CZ-128 40 Prague 2, Czech Republic, European Union
[f] Department of Paediatric Haematology and Oncology, 2nd Faculty of Medicine, Charles University, and University Hospital Motol, V Uvalu 84, CZ-150 06 Prague 5, Czech Republic. European Union
* E-mail: kizek@sci.muni.cz

2. Experimental

2.1 Chemicals

ETO, citric acid, PVP with a molecular mass of 10 kg mol^{-1}, ethylene glycol, methanol (MeOH) and others were purchased from Sigma-Aldrich Co. (St. Louis, MO, USA) unless stated otherwise. AD-TUBE Dialyzer maxi MWCO 3.5 kDa was bought from EMD Millipore Corporation (San Diego, CA, USA). Deionized water underwent demineralization by reverse osmosis using an Aqua Osmotic 02 (Aqua Osmotic, Czech Republic) and was subsequently purified using a Millipore RG (Milli-Q water, 18 M, Millipore Corp., Billerica, MA, USA).

2.2 Preparation of CQDs

Synthesis of CQDs capped with PVP was conducted by pyrolyzing the mixture of citric acid and PVP according to the method described in our previous study.[44] Briefly, 1.00 g of citric acid and 1.00 g of PVP were dissolved in a 100 mL three neck flask with 20.0 mL of ethylene glycol and then heated moderately using a heating mantle (200 °C), for 3 h under nitrogen flow, and then cooled down to ambient temperature. Milli-Q water was then added and the mixture was stirred for a couple of minutes. The obtained solution was purified for 24 h by dialysis against Milli-Q water with a D-Tube maxi dialyzer to remove ethylene glycol.

2.3 Preparation of modified GCE electrode

Before modifying the electrode surface, its surface was carefully polished with 0.1 µm alumina powder (ESA Inc., Chelmsford, MA, USA) and ultra-sonicated in Sonorex digital 10 P ultrasonic bath (Bandelin, Berlin, Germany) for 15 min in Milli-Q water. Then, the GCE was modified by 3 different ways. (i) Firstly, GCE was immersed in CQDs solution (labelled with GCE-CQDs) and then that modified GCE was employed to measure ETO. (ii) The second way was the physicochemical adsorption of CQDs on the surface of working electrode. Briefly, 5.0 µL of CQDs were placed on the electrode surface followed by a hair drying method till ready to use for measurements of ETO (labelled with GCE/CQDs). (iii) The third way exploited continual physicochemical adsorption of ETO on the surface of GCE/CQDs followed by measuring of ETO (labelled with GCE/CQDs/ETO).

Effect of deposition potential and deposition time of ETO measured by the second way was also tested in the present study.

2.4 Electrochemical detection

Electrochemical detection of ETO was carried out using µAutolab (Metrohm, Herisau, Switzerland) with glass cell and three electrodes. Ag/AgCl/3M KCl was used as a reference electrode and platinum as an auxiliary electrode. A GCE (diameter 3 mm) modified with CQDs was used as the working electrode. Differential pulse voltammetry (DPV) and cyclic voltammetry (CV) were performed in the presence of Britton-Robinson (BR) buffer (pH = 6.0) at room temperature. The parameters for differential pulse voltammetry were: initial potential 0.0 V, end potential 1.0 V, step potential 5 mV, modulation amplitude 0.1 V and modulation time 4 ms, interval time 0.1 s. The parameters for cyclic voltammetry were: start potential 0.10 V, upper vertex potential 0.65 V, lower vertex potential 0.10 V, stop potential 0.10 V, number of stop crossing 2, step potential 0.10 V, scan rate 0.05 V s^{-1}, potential step 5 mV, modulation amplitude 0.025 V and modulation time 0.05 s.

2.5 Electrochemical impedance spectroscopy (EIS) measurement

EIS were carried out using a standard three-electrode system at 25 °C. The reference electrode was an Ag/AgCl/3M KCl electrode and platinum wire was used as the counter electrode (CH Instruments, Austin, TA, USA). GCE with 3 mm in diameter (CH Instruments) was used to determine formal potential of $[Fe(CN)_6]^{3-}$ reduction. In order to it, cyclic voltammograms (scan rate 0.05 V s^{-1} in potential range (−0.3 – +0.7 V)) were measured in the presence of 2 mM $K_3[Fe(CN)_6]/K_4[Fe(CN)_6]$ (1:1) solution in 0.1 M KCl (pH 7). The formal potential was subsequently used as the potential of EIS measurement (AC amplitude 0.01 V, range 0.1 – 10^3 Hz). The same procedure was performed with GCE/CQDs and GCE/CQDs/ETO. The signals were recorded using potentiostat PGSTAT302N (Metrohm, Herisau, Switzerland) with a frequency response analyser and evaluated using software NOVA 1.8 (Metrohm, Herisau, Switzerland). Before modification and measurement, the GCE was mechanically polished by the 0.1 µm alumina suspension on a polishing cloth to produce mirror-like surface. Then, the electrode was sonicated for 1 min in acetone and deionised water (25 °C) in the ultrasonic bath, respectively.

2.6 Cell culture

PC3 a human cell line established from a grade 4 androgen independent prostatic adenocarcinoma was purchased from Health Protection Agency Culture Collection (Salisbury, UK). The cells were grown in the Ham´s 12 medium with 7% foetal bovine serum (*v*/*v*, FBS) supplemented with penicillin (100 U mL^{-1}) and streptomycin (0.1 mg mL^{-1}). The cells were maintained at 37 °C in a humidified incubator (Sanyo, Moriguchi, Japan) with 5% CO_2. The treatment was carried out once the cells reached 50 – 60% confluence.

2.7 Administration by ETO and cytotoxicity testing

The suspension of 5 000 cells was added to each well of standard microtiter plates (E-plates 16). After the addition of the medium (200 µL), the plates were incubated for 2 days at 37 °C to ensure cell growth. Consequently, the existing medium was replaced by a fresh medium containing ETO (1 – 500 µM) and a medium without ETO as a control. The plates were incubated for 24 h; then, the medium was removed and replaced by a fresh one, three times a day. Further, the medium was replaced by 200 µL of the fresh medium containing 50 µL of 3-(4,5-dimethylthiazol-2-yl)-2,5-diphenyltetrazolium bromide (MTT, 5 mM in PBS) and incubated in a humidified atmosphere for 4 h at 37 °C, and wrapped in an aluminium foil. After the incubation, the MTT-containing medium was replaced by 200 µL of 99.9% dimethyl sulfoxide to dissolve MTT-formazan crystals. Then, 25 µL of glycine buffer was added to all wells and the absorbance was immediately determined at 570 nm (VersaMax microplate reader, Molecular Devices, Sunnyvale, CA, USA).

2.8 Microscopic examination

For light microscopy, the cells were cultivated directly on glass microscopic slides (75 × 25 mm, thickness 1 mm, Fischer Scientific, Pardubice, Czech Republic) in Petri dishes in the above mentioned cultivation medium as described in cell culture conditions. Following treatment, the glass microscope slides with a monolayer of cells were removed from the Petri dishes, rinsed with a cultivation medium and PBS buffer and directly used for light microscopy under an inverted microscope (Eclipse TS100; Nikon, Tokyo, Japan). The images were taken using a digital camera (Nikon D3300, Nikon, Tokyo, Japan).

2.9 Preparation of cell samples for electrochemical detection and HPLC-ED analysis

A prostate cancer cell line, PC3 which is commonly used in biomedical research, was selected. Approximately 1000 cells were incubated in 100 µL of a reduced serum medium for the cell culture (Opti-MEM, Life Technologies, CA, USA) maintaining slandered conditions (37 °C, 5% CO_2) in an incubator (New Brunswick Eppendorf, Hamburg, Germany). The ETO solution was added to the cells in a final concentration of 200 µM. After different times of incubation (1, 3, 6, 9, 12, 18 and 24 h), these samples were prepared by two different ways for electrochemical detection and HPLC-ED, respectively.

Cell samples for electrochemical detection were washed 3 times with same medium to remove extra ETO from the medium. After the washing, the cells were re-suspended in 100 µL of the same medium. To detect ETO in the cytosol, the cell membranes were disrupted by 5 min long sonication. The cell suspension was then measured using both bare GCE and GCE/CQDs.

Cell samples for HPLC-ED, were deproteinized using 40 µL of 10% TFA (*v/v*) and centrifuged using Microcentrifuge 5417R (Eppendorf AG, Hamburg, Germany) under 25 000 × *g* at 4 °C for 15 min. The obtained supernatant was analysed using HPLC-ED.

2.10 Descriptive statistics

Mathematical analysis of the collected data and their graphical interpretation were performed by Microsoft Excel®, Microsoft Word® and Microsoft PowerPoint®. Results are expressed as mean ± standard deviation (S.D.) unless noted otherwise. The detection limits (3 signal/noise, S/N) and quantification limits (10 signal/noise, S/N) were calculated according to Long and Winefordner,[45] whereas N was expressed as standard deviation of noise determined in the signal domain unless stated otherwise.

Further information about other methods can be found in the supplymentary file.

3. Results and discussion

3.1 Characterization of CQDs

Fig. 1SA1 shows size distribution of CQDs under different pH. The particle size measurements revealed moderate changes in particle sizes within the pH range from 2 to 9 (Fig. 1SA2). Within this pH range, the samples consisted in almost monodisperse system with particle sizes varying from less than 1 to 2.5 nm. With the increase of the pH from 2 to 5, the size of particles decreases probably due to the shifting of the electric double layer absorption/desorption equilibrium toward the last one and the diminishing of the Colombian mutual attraction between particles. With further increase in the pH from 5 to 8, the particles are partially negatively charged due to the carboxylic groups from attached moieties of citrate, which enable the formation of bigger micelles. Anyway, this phenomenon is reversed with the enhancement of the pH form 8 to 9 due to the cationic saturation of the surface double layer around CQDs. Consequent zeta potential measurements (Fig. 1SA3) revealed a slight increase of zeta potential when increasing the pH from 2 to 3 exhibited by the cationic exchange capacity of the double layer leading to enhanced density of cations on the surface of the particles. Further pH increase rises the concentration of the phosphate ions, which lead to continuous decrease in zeta potential toward negative values, until −3.5 mV, obtained for pH = 8. Once this double layer is saturated with phosphate ions, further increase in the pH contributes to attraction of the cations present in the solution, decreasing therefore the excess of negative charges around the CQDs and therefore contributing to the obvious increase in the zeta potential. The latter is in full agreement to the decrease in the particle size (Fig. 1SA3).

Fluorescence intensity and absorbance of different concentrations of CQDs were also determined. Fig. 1SB1 and 1SB2 showed dependence of fluorescence intensity and absorbance on concentration of CQDs. It can be seen that fluorescence intensity and absorbance increased with the increasing concentration of CQDs. Insets in Fig. 1SB1 and 1SB2 show fluorescence and absorbance spectra of CQDs.

3.2 Electrochemical detection of ETO using bare GCE

The mechanism of electro-oxidation of the 2,6-dimethoxyphenol group of ETO using GCE[36, 46] and carbon paste electrode[20] has been presented. In this study, CV and DPV methods were used for detection of ETO. Fig. 1 demonstrates CV and DPV analysis of ETO measured by bare GCE. Fig. 1 A1 shows typical cyclic voltammogram of ETO including oxidation and reduction peak. Phosphate and BR buffer with different pHs were employed for determination of ETO. Fig. 1 A2 and A3 present dependence of peak height and potential on pH of phosphate and BR buffer, respectively. In the presence of phosphate buffer, both oxidation and reduction peak decreased with the increasing pH up to 7 and then increased at pH 8. In the presence of BR buffer, both oxidation and reduction peak increased according to the increase of pH up to 6 and then started to decrease when pH increased from 7 to 11. In both above figures, changing of pH does not strongly influence the peak position. As it can be seen from these figures, BR buffer at pH 6 gave the best environment for obtaining the highest signal. Therefore, this condition was further used for determination dependence of a scan rate on oxidation and reduction peak height (Fig. 1 A4). It is obvious that both signals increased with the increasing scan

rate. Similarly, Fig. 1 B1 shows the differential pulse voltammetric behaviour of ETO. The position of the peak was 0.42 V. Phosphate and BR buffers with different pH were also used for determination of ETO by this electrochemical method. The response of ETO signal in this case is the same with oxidation peak of ETO measured by CV, which is showed in Fig. 1 B2 and B3. However, position of the ETO signal measured by DPV shifted to the negative potential direction when pH of BR buffer increased. BR buffer of pH 6 also gave the highest signal (Fig. 1 B3) and was used to measure the dependence of step potential on ETO peak height, which is shown in Fig. 1 B4. It clearly follows from the results obtained that ETO signal increased according to the increase in step potential. Furthermore, step potential does not affect the peak position. In comparison with CV, DPV produced a higher oxidation signal of ETO. Therefore, DPV under the optimized pH buffer and step potential were chosen for the calibration curve of ETO determination as well as for ETO measurements on modified GCE. The calibration curve presented in Fig. 2 A is characterised by the equation $y = 0.0355x - 0.0016$ with $R^2 = 0.9965$. The analytical parameters for electrochemical detection of ETO measured by bare GCE are shown in Tab. 1. Linear dynamic range is 0.06 – 100 µM. The estimated limit of detection (LOD) and the limit of quantification (LOQ) were 0.017 and 0.057 µM, respectively.

Fig. 1: CV and DPV analysis of ETO (200 µM) measured by GCE (column: peak height or relative peak height, square dot: potential). (A1) Cyclic voltammograms of buffer and ETO. Dependence of peak (reduction and oxidation) height of ETO and potential on pH of (A2) phosphate and/or (A3) BR buffer measured by CV (A2, A3). (A4) Dependence of oxidation and reduction peak height on scan rate measured by CV in BR buffer pH 6. (B1) Differential pulse voltammograms of buffer and ETO. Dependence of peak height and potential on pH of (B2) phosphate and (B3) BR buffer measured by DPV. (B4) Dependence of relative peak height and potential on step potential measured by DPV in BR buffer pH 6. Parameters for CV analysis: start potential −0.1 V, upper vertex potential 0.6 V, lower vertex potential −0.1 V, stop potential −0.1 V, number of stop crossings 2, step potential 2.5 mV. Parameters for DPV analysis: initial potential 0.0 V, end potential 1.0 V, step potential 5 mV modulation amplitude 0.1 V, modulation time 4 ms, interval time 0.1 s.

Fig. 2: Calibration curve of ETO measured by bare GCE (A) and GCE/CQDs using DPV method under optimized conditions.

Tab. 1 Comparison of the analytical parameters for the detection of ETO using different methods.

Method	*Working Electrode*	*Regression equation*	*Linear dynamic range (µM)*	*$R^{2a)}$*	*$LOD^{b)}$ (µM)*	*$LOQ^{c)}$ (µM)*	*RSD (%)*	*Ref.*
Electrochemistry	Bare GCE	y = 0.0355x – 0.0016	0.06 – 100	0.9965	0.017	0.057	4.81	
Electrochemistry	GCE/CQDs	y = 0.4376x + 0.0592	0.02 – 10.0	0.9983	0.005	0.016	5.26	
Electrochemistry	Carbon paste electrode	y = 0.29436x + 0.58165	0.25 – 10.0	0.9983	0.100	---	2.77	20
Electrochemistry	GCE modified with multi-walled CNT	y = 1.696x + 0.015	0.02 – 2.00	0.9980	0.005	0.018	0.73	36
FIA		y = 0.7282x + 0.2145	0.11 – 6.00	0.9947	0.032	0.108	5.19	

[a] Regression coefficient.
[b] LOD (S/N=3).
[c] LOQ (S/N=10).

--- This was not mentioned.

3.3 FIA-ED of ETO

Based on the convincing results obtained from stationary electrochemistry, we decided to test the behaviour of ETO in flow arrangement. Flow injection analysis (FIA) setup equipped with an electrochemical detector (ED) containing four analytical cells was employed for detection of ETO. Firstly, electrochemistry was utilized to monitor an effect of organic solvents in mobile phase on an electrochemical response of ETO. As it can be seen in Fig. 2SA, two organic solvents (MeOH and ACN) were tested in 3% addition (*v/v*) into 80 mM TFA with pH 1.5 used as a mobile phase. The analysis was performed within the potential range from 500 to 1100 mV, and it was shown that ACN supports the analysis at an ideal potential (1100 mV), which is above that of MeOH (peak height of ETO for ACN 37.33 µA and for MeOH 33.99 µA). Therefore, 3% addition of ACN to TFA (*v/v*) was chosen as beneficial to increase sensitivity in subsequent analyses.

Although TFA with 3% addition of ACN showed relatively good detector response of ETO, we decided to test various pH buffers due to their ability to enhance the sensitivity of detection. Firstly, we tested various pH values of BR buffer, whereas BR buffer was shown to have the greatest effect on peptide and doxorubicin detection based on our previous study.[47, 48] Hence, for further optimization experiments we utilized merely BR buffer in pH range of 3 – 8 (3% addition of ACN (*v/v*)) and potentials within the range from 100 to 1100 mV (Fig. 2SB). Fig. 2SB makes it obvious, a low pH value, maintained by BR buffer with pH 3, was shown to influence the sensitivity of detection of ETO. The ideal potential was found at 1100 mV showing ETO peak with height of 20.10 µA. After application of BR buffer with pH 4 it was shown that ideal potential was found at 1100 mV (peak height 22.3 µA) and the same phenomenon was observed at BR buffer with pH 5 (peak height 33.9 µA). Interestingly, at pH 6 a significant change in electrochemical behaviour of ETO occurred. In this case, the ideal potential was determined at 1100 mV (peak height 40.06 µA) and the same trend was observed at all of BR buffer pHs used in this study (pH 7 – peak height 42.03 µA, pH 8 – peak height 41.93 µA). Based on the obtained data it is obvious that BR buffer with pH 7 shows the most beneficial effect on ETO, and therefore we decided to use it as mobile phase for subsequent analyses.

Using the ideal conditions found from previous experiments (BR buffer with pH 7, with 3% addition of ACN (*v/v*)) we carried out further analysis to obtain hydrodynamic voltammogram (HDV) of ETO. Hence, for further optimization experiments we utilized merely BR buffer in pH 7 (3% addition of ACN (*v/v*)) and potentials 1100 mV while using different temperature ranging between 25 – 35 °C (Fig. 2SC). The ideal temperature was determined at 30 °C (Fig. 2SC). Moreover, the working electrode should be immersed to the supporting electrolyte and should give response only to the analysed substance in a thermodynamically defined, potential-dependent fashion.[49] In our case hydrodynamic voltammetry was carried out within the potential range from 100 to 1100 mV (Fig. 2SD). It clearly follows from the results obtained

that the current response increases relatively slowly up to reaching interval of redox potential (800 mV). After reaching this "inflection point", the current response increases rapidly to high oxidation potential, where maximal detection potential (1100 mV) was achieved as the ideal for ETO determination.

After the optimization of the electrochemical analysis for the ETO, the calibration curve was recorded within the range from 0.11 to 6.00 µM. The array record obtained from calibration curve measurements is shown in Fig. 2SE. The collected data are plotted in the calibration curve shown by the inset in Fig. 2SE. For concentrations above the mentioned range, linear dependence of ETO signal on its applied concentration ($y = 0.7282x + 0.2145$, $R^2 = 0.9947$) was obtained. Using the optimal conditions, we were able to estimate the detection limit of ETO as 0.032 µM. A limit of quantification was estimated as 0.108 µM. Further analytical parameters are shown in Tab. 1. In comparison with electrochemical detection using bare GCE, it can be concluded that electrochemical detection is more sensitive than FIA method due to lower LOD and LOQ.

3.4 Study of bare GCE, GCE/CQDs, and GCE/CQDs/ETO using SEM, FM, and EIS

Fig. 3A1, A2, and A3 show SEM images of bare GCE, GCE/CQDs, and GCE/CQDs/ETO, respectively. The surface of freshly polished bare electrode is smooth without observable impurities or defects even at magnification 3000 × (Fig. 3A1). GCE/CQDs bears on its surface clearly visible conglomerates of CQDs (Fig. 3A2), which are responsible for the increased sensitivity of the modified electrode. Conglomerates of CQDs have from 2 to 4 µm in diameter, thus they are approximately a thousand times greater than CQDs themselves. It can be estimated that one of such conglomerates was formed from several thousands (3 – 6 thousands approximately) of CQDs (close-packing of equal spheres expected). Fig. 3A3 (GCE/CQDs/ETO) illustrates that ETO layer covered the conglomerates of CQDS. Therefore, some conglomerates of CQDs are visible only.

The presence of CQDs on GCE and its fluorescent property were studied by fluorescence microscopy (Fig. 3B2). The GCE was placed in an inverted position on the objective lens. It clearly follows from the results obtained that there is no fluorescence on the bare GCE before modification (Fig. 3B1) except a tiny sharp round line, which comes from the uneven joining border line of the glassy carbon (GC) and the covering rubber. After the modification with CQDs, a very bright fluorescence was observed at the centre of the electrode, which proves the presence of sufficient amount CQDs on the GCE (Fig. 3B2). However, the GCE lost its fluorescence after the interaction with ETO probably because the anticancer drug was able to cover all of the CQDs present on the modified GCE (Fig. 3B3). The results from SEM and FM indicated the successful modification of GCE with CQDs. Furthermore, different surfaces between GCE/CQDs and GCE/CQDs/ETO can lead to the different electrochemical signal of ETO.

Fig. 3: (A) SEM and (B) FM images of bare GCE (A1, B1), GCE/CQDs (A2, B2), GCE/CQDs/ETO (A3, B3). SEM images were recorded with a magnification 20 µm and an accelerating voltage of 15 kV.

In order to elucidate the effect of CQDs on the properties of electrode, the electrochemical impedance spectra of bare GCE were compared with spectra of GCE modified with CQDs (GCE/CQDs) covered with PVP. As exhibited by the Nyquist plot in Fig. 4, the presence of CQDs on the surface of an electrode decreased the rate of the electron transfer (increased the resistivity of the system). In general the Nyquist plot is composed of two parts, where the semi-circle in higher frequencies or more precisely its diameter represents the charge transfer resistance and the linear part with a slope app. 0.5 represents the diffusion of reduction probe to the surface of an electrode. The presence of CQDs on the electrode resulted in the decrease of oxidation and reduction signals by 33 % causing increase also in peak-to-peak separation by 0.19 V to 0.31 V. Modified Randles' equivalent circuit composed of electrolyte resistance R_e, double layer capacitance C_{dl}, charge transfer resistance R_{ct} and Warburg element Z_W was used to calculate the properties of GCE. The charge transfer resistance of 1.84 kΩ was calculated for GCE. For fitting the modified electrode the equivalent circuit depicted in the bottom inset in Fig. 4 was used. It consisted of the following parts: electrolyte resistance R_e, with in series resistance of CQDs R_l and constant phase element CPE ($Z_{CPE} = 1/j(\omega Q)^n$) representing CQDs layer, charge transfer resistance R_{ct}, double layer capacitance C_{dl} and Warburg element Z_w. To obtain the best fitting results the capacitor was in one case replaced by CPE nevertheless its n is 0.79 and the CQDs layer can be considered as a capacitive. We obtained charge transfer resistance of GCE/CQDs 3.47 kΩ. Subsequently, the GCE/CQDs were modified with ETO (GCE/CQDs/ETO) and CV and EIS were measured using this modified electrode. After modification with ETO the oxidation and reduction signal of $[Fe(CN)_6]^{3-/4-}$ increased by 7% in comparison with GCE/CQDs (insert in Fig. 4). Nevertheless the peak separation increased again. In the case of EIS the R_{CT} of GCE/CQDs/ETO decreased to 3.25 kΩ. It can be concluded that resistivity of bare GCE, GCE/CQDs, and GCE/CQDs/ETO are different, which can cause the change in electrochemical signal of ETO.

Fig. 4. The electrochemical impedance spectra of bare GCE (blue line), GCE/CQDs (green line), GCE/CQDs/ETO (red line). Upper insert shows cyclic voltammograms of bare GCE (blue line), GCE/CQDs (green line), GCE/CQDs/ETO (red line) in supporting electrolyte. Bottom insert shows Randles' equivalent circuit schematic using modified GCE. Concentration of ETO is 200 µM. Supporting electrolyte: a 1:1 solution of 0.2 M KCl containing 2.0 mM $[Fe(CN)_6]^{3-/4-}$.

3.5 Electrochemical detection of ETO using GCE modified with CQDs

Three different ways of modifying the surface of GCE with CQDs were tested in this study. Fig. 5 A, B and C show dependence of relative ETO peak height on concentration of CQDs measured by GCE-CQDs, GCE/CQDs, and GCE/CQDs/ETO, respectively. With GCE-CQDs, ETO signal decreased after modifying working electrode. It slightly increased with the increasing concentrations of CQDs up to 30 µM and then decreased down to 500 µM. A second way of modifying GCE (GCE/CQDs) showed positive results due to concentrations of CQDs ranging 0.25 to 8.0 µM. In this case, ETO signal highly increased in comparison with bare GCE. The best concentration of CQDs was found to be 4.0 µM. However, from 8.0 to 500 µM concentration of CQDs peak of ETO decreased. The last way of modification GCE (GCE/CQDs/ETO) did not enhance the ETO signal, which can be seen in Fig. 5C. With concentrations of CQDs ranging from 0.25 to 25 µM, ETO signal increased and then start to decrease down to 500 µM. It can be concluded that for electrochemical sensing of ETO, GCE/CQDs presented the best result because it increases significantly the ETO signal in comparison to bare electrode. Therefore, this method was used to measure calibration curve of ETO (Fig. 2B). Moreover, LOD and LOQ of that new method for detection of ETO were estimated, which is shown in Tab. 1. It can be seen that sensitivity of a method using GCE/CQDs is better than using bare GCE because by using GCE/CQDs, LOD and LOQ both decreased 3.4 times. According to our knowledge, GCE/CQDs produced lowest LOD for electrochemical determination of ETO in comparison with previous publications, which is shown in Tab. 1.

Furthermore, this method was also employed to test the effect of deposition potential and deposition time of ETO on ETO signal. Fig. 5D shows dependence of deposition potential of ETO on relative ETO peak height and potential measured by GCE/CQDs. ETO signal increased from deposition potential of 0.0 to 0.2 V and then start to linearly decrease down to 1.2 V. The dependence of deposition time of ETO on relative peak height and potential is shown in Fig. 5E. ETO signal increased with the increasing deposition time up to 90 s and then decreased down to 180 s. Furthermore, deposition potential and deposition time of ETO does not strongly effect the position peak of ETO measured by GCE/CQDs.

Fig. 5 Differential pulse voltammetry analysis of ETO (10 µM) measured by GCE modified with CQDs (column: peak height or relative peak height, triangle: potential). (A) Dependence of relative peak height of ETO on concentration of CQDs measured by GCE-CQDs. (B) Dependence of relative peak height of ETO on concentration of CQDs measured by GCE/CQDs (blue star corresponds to at least 10% ETO signal increase measured by GCE/CQDs compared with bare GCE). (C) Dependence of relative peak height of ETO on concentration of CQDs measured by GCE/CQDs/ETO. (D) Dependence of relative peak height and potential on deposition potential of ETO measured by GCE/CQDs. (E) Dependence of relative peak height and potential on deposition time of ETO measured by GCE/CQDs. Parameters for DPV analysis: initial potential 0.0 V, end potential 1.0 V, step potential 40 mV, modulation amplitude 0.1 V, modulation time 4 ms, interval time 0.1 s.

3.6 Determination of ETO concentrations in ETO-treated cancer cell

Firstly, PC3 cancer cells were administered to the increasing concentration of ETO to determine its cytotoxic effects. Fig. 6A1 illustrates significant toxicity of drug within tested cells. Furthermore, IC_{50} was established to be 22.5 µM. As ETO is described apoptosis inducer[50], we employed light microscopy to determine the major apoptosis characteristics in treatment time-course. Untreated cells (Fig. 6A2) exhibit adherent monolayer forming clusters in their colony. After 5 h long administration, characteristic morphological changes related to apoptosis such as the presence of apoptotic bodies, condensation of chromatines, cell shrinkage and shape changes were found (Fig. 6A3). These apoptotic features were more visible in the experiment end-point (24 h) with higher amount of cell blebs localized in cytoplasm as a result of zeiosis (Fig. 6A4). The obtained results confirmed the action of ETO and its presence in cells, subsequently processed for further analyses.

Electrochemical detection (bare GCE and GCE/CQDs) and HPLC-ED were employed to measure ETO administered by cancer cells. Fig. 6B shows the dependence of ETO peak height on exposure time of ETO into the cancer cells measured by GCE and GCE/CQDs. It was found that the amount of the ETO in the cytosol of the PC3 cells gradually increased with the increasing time of incubation and after 9 h only moderate increase of the signal was found probably because the cellular uptake of ETO came close to saturation. Furthermore, peak heights measured by GCE/CQDS were all significantly higher than measured by bare GCE ($p < 0.05$). Fig. 6C presents dependence of a peak area obtained using HPLC-ED on exposure time of ETO. The same phenomena were observed when ETO signal increased up to exposure time of 9 h and then slightly increased.

Concentrations of ETO in cancer cells were calculated from both methods (Fig. 6D). Results from both methods fitted well. Electrochemistry (GCE/CQDs) showed higher calculated concentrations of ETO in comparison with HPLC-ED, whereas Fig. 6E presents correlation between two methods for determination of ETO into the cancer cell.

Fig. 6 (A1) Testing of cytotoxicity of ETO on PC3 prostate cancer cells using MTT assay, with inserted IC_{50}. Determination of ETO effects *via* light microscopy, showing (A2) untreated PC3 cells and the same cells treated with 10 µM of ETO. Images were acquired after (A3) 5 h and (A4) after 24 h. The length of scale bar is 50 µm. Arrows indicate some typical morphological features, resulting from apoptosis (blue arrows are rounded shape of cells, green arrows are condensation of chromatin or red arrows are apoptotic bodies). Detection of ETO after applying into the PC3 cancer cells measured by electrochemical detection and HPLC-ED. (B) Dependence of peak height on exposure time of ETO into the cancer cell measured by bare GCE and GCE/CQDs. (C) Dependence of

peak area on exposure time of ETO measured using HPLC-ED. (D) Dependence of concentration of ETO on exposure time of ETO measured by HPLC-ED and GCE/CQDs. (E) Correlation between HPLC-ED and GCE/CQDs for determination of ETO in cancer cells after 1, 3, 6, 9, 12, 18, and 24 h of exposure time. Asterisks indicate significant differences ($p < 0.05$).
Further information about other figures can be found in the supplymentary file.

4. Conclusion

A novel pioneering study was performed using the advantageous characteristics of nano dimensions CQDs for modification GCE. It reveals that ETO signal increases of app. 34% in comparison to the bare GCE, thus we reached the increasing the sensitivity of developed method. This is the most sensitive method for determination of ETO with the lowest LOD compared with previously published electrochemical methods. Furthermore, our novel approach was employed to analyse real samples represented by PC-3 cancer cells treated with the drug of the interest. It was found that the amount of the ETO in the cytosol of the PC3 cells was gradually increased according to the increase of incubation time and after 9 h only slight elevation in the signal was seen probably due to the saturation of the cellular uptake of ETO. Moreover, this phenomenon was also confirmed by using HPLC-ED technique.
Besides, three different ways of modifying GCE with CQDs were presented in this study and can be employed to test the efficiency of each modification way to differences kind of samples such as heavy metals, other anticancer drugs, and/or other biological samples. The mechanisms of the difference among these three ways corresponding to different kinds of samples are prone of further investigations.

Acknowledgements

Financial support by GA CR (NANOCHEMO 14-18344S) and from the Ministry of Health of the Czech Republic for conceptual development of research organization 00064203 (University Hospital Motol, Prague, Czech Republic) are highly acknowledged.

Notes and references

1. S. Maghsoudi and E. Noroozian, *Chromatographia*, 2012, **75**, 913-921.
2. Z. G. Yu, Z. Qin, H. R. Ji, X. Du, Y. H. Chen, P. Pan, H. Wang and Y. Y. Liu, *Chromatographia*, 2010, **72**, 1073-1081.
3. I. Blazkova, H. V. Nguyen, M. Kominkova, R. Konecna, D. Chudobova, L. Krejcova, P. Kopel, D. Hynek, O. Zitka, M. Beklova, V. Adam and R. Kizek, *Electrophoresis*, 2014, **35**, 1040-1049.
4. A. C. Tripathi, S. A. Saraf and S. K. Saraf, *Materials*, 2015, **8**, 3068-3100.
5. T. Yamashita, K. Yamashita, H. Nabeshi, T. Yoshikawa, Y. Yoshioka, S. Tsunoda and Y. Tsutsumi, *Materials*, 2012, **5**, 350-363.
6. M. Pumera, *ACS Nano*, 2014, **8**, 7555-7558.
7. P. Greil, *Adv. Eng. Mater.*, 2015, **17**, 124-137.
8. M. Pumera, *J. Mater. Chem. C*, 2014, **2**, 6454-6461.
9. Y. Q. Dong, J. H. Cai, X. You and Y. W. Chi, *Analyst*, 2015, **140**, 7468-7486.
10. S. X. Chen, F. W. Li, C. H. Fan and S. P. Song, *Analyst*, 2015, **140**, 6439-6451.
11. X. Y. Sun, P. C. Liu, L. L. Wu and B. Liu, *Analyst*, 2015, **140**, 6742-6747.
12. S. N. Baker and G. A. Baker, *Angew. Chem.-Int. Edit.*, 2010, **49**, 6726-6744.
13. D. Fernandes, M. J. Krysmann and A. Kelarakis, *Chem. Commun.*, 2015, **51**, 4902-4905.
14. J. H. Shen, Y. H. Zhu, X. L. Yang and C. Z. Li, *Chem. Commun.*, 2012, **48**, 3686-3699.
15. L. L. Li, G. H. Wu, G. H. Yang, J. Peng, J. W. Zhao and J. J. Zhu, *Nanoscale*, 2013, **5**, 4015-4039.
16. Y. C. Song, D. Feng, W. Shi, X. H. Li and H. M. Ma, *Talanta*, 2013, **116**, 237-244.
17. S. K. Pang, N. Y. Zheng, C. A. Felix, J. Scavuzzo, R. Boston and I. A. Blair, *J. Mass Spectrom.*, 2001, **36**, 771-781.
18. T. Groh, J. Hrabeta, J. Poljakova, T. Eckschlager and M. Stiborova, *Neuroendocrinol. Lett.*, 2012, **33**, 16-24.
19. Z. Heger, A. Moulick, V. H. Nguyen, M. Kremplova, P. Kopel, D. Hynek, T. Eckschlager, M. Stiborova, O. Zitka, V. Adam and R. Kizek, *Int. J. Electrochem. Sci.*, 2015, **10**, 7707-7719.
20. A. E. Radi, N. Abd-Elghany and T. Wahdan, *Chem. Pharm. Bull.*, 2007, **55**, 1379-1382.
21. B. S. Glisson and W. E. Ross, *Pharmacol. Ther.*, 1987, **32**, 89-106.
22. H. Hu, Z. Q. Wang, S. Y. Liu, Y. C. Cheng and K. H. Lee, *J. Med. Chem.*, 1992, **35**, 866-871.
23. Y. L. Zhang, Y. C. Shen, Z. Q. Wang, H. X. Chen, X. Guo, Y. C. Cheng and K. H. Lee, *J. Nat. Prod.*, 1992, **55**, 1100-1111.
24. P. Darpa and L. F. Liu, *Biochim. Biophys. Acta*, 1989, **989**, 163-177.
25. Y. Pommier, G. Capranico, A. Orr and K. W. Kohn, *J. Mol. Biol.*, 1991, **222**, 909-924.
26. M. Roberge, J. Thng, J. Hamaguchi and E. M. Bradbury, *J. Cell Biol.*, 1990, **111**, 1753-1762.
27. X. J. Cai, M. J. Woo, M. J. Edick and M. V. Relling, *J. Chromatogr. B*, 1999, **728**, 241-250.
28. Y. Kato, H. Mawatari, S. I. Nishimura, N. Sakura and K. Ueda, *Acta Med. Okayama*, 2003, **57**, 21-24.
29. R. Saadati, S. Dadashzadeh and F. M. Shahab, *Eur. J. Pharm. Sci.*, 2009, **38**, 182-183.
30. L. Skibinska, *Chemia Anal.*, 2001, **46**, 849-855.
31. M. Snehalatha, B. Girish, K. Venugopal and R. N. Saha, *Indian J. Pharm. Educ. Res.*, 2007, **41**, 347-352.
32. R. Zhou, M. Frostvik-Stolt and E. Liliemark, *J. Chromatogr. B*, 2001, **757**, 135-141.
33. R. J. Strife, I. Jardine and M. Colvin, *J. Chromatogr.*, 1981, **224**, 168-174.
34. J. Tuerk, T. K. Kiffmeyer, C. Hadtstein, A. Heinemann, M. Hahn, H. Stuetzer, H. M. Kuss and U. Eickmann, *Int. J. Environ. Anal. Chem.*, 2011, **91**, 1178-1190.
35. N. Y. Ragozina, M. Putz, S. Heissler, W. Faubel and U. Pyell, *Anal. Chem.*, 2004, **76**, 3804-3809.

36. B. Bozal-Palabiyik, B. Dogan-Topal, B. Uslu, A. Can and S. A. Ozkan, *J. Solid State Electrochem.*, 2013, **17**, 2815-2822.
37. A. E. Radi, H. M. Nassef and A. Eissa, *Electrochim. Acta*, 2013, **113**, 164-169.
38. Y. H. Yang, J. H. Cui, M. T. Zheng, C. F. Hu, S. Z. Tan, Y. Xiao, Q. Yang and Y. L. Liu, *Chem. Commun.*, 2012, **48**, 380-382.
39. J. Y. Yin, H. J. Liu, S. Z. Jiang, Y. Chen and Y. F. Yao, *ACS Macro Lett.*, 2013, **2**, 1033-1037.
40. M. Zheng, S. Liu, J. Li, D. Qu, H. F. Zhao, X. G. Guan, X. L. Hu, Z. G. Xie, X. B. Jing and Z. C. Sun, *Adv. Mater.*, 2014, **26**, 3554-3560.
41. Y. Q. Dong, R. X. Wang, H. Li, J. W. Shao, Y. W. Chi, X. M. Lin and G. N. Chen, *Carbon*, 2012, **50**, 2810-2815.
42. B. Liao, P. Long, B. Q. He, S. J. Yi, B. L. Ou, S. H. Shen and J. Chen, *J. Mater. Chem. C*, 2013, **1**, 3716-3721.
43. F. Wang, Z. Xie, H. Zhang, C. Y. Liu and Y. G. Zhang, *Adv. Funct. Mater.*, 2011, **21**, 1027-1031.
44. V. Milosavljevic, H. V. Nguyen, P. Michalek, A. Moulick, P. Kopel, R. Kizek and V. Adam, *Chem. Pap.*, 2015, **69**, 192-201.
45. G. L. Long and J. D. Winefordner, *Anal. Chem.*, 1983, **55**, A712-724A.
46. J. J. M. Holthuis, W. J. Vanoort, F. M. G. M. Romkens, J. Renema and P. Zuman, *J. Electroanal. Chem.*, 1985, **184**, 317-329.
47. M. Kominkova, R. Guran, M. A. R. Merlos, P. Kopel, I. Blazkova, D. Chudobova, L. Nejdl, Z. Heger, B. Ruttkay-Nedecky, O. Zitka, V. Adam and R. Kizek, *Int. J. Electrochem. Sci.*, 2014, **9**, 2993-3007.
48. N. Cernei, Z. Heger, P. Kopel, V. Milosavljevic, M. Kominkova, A. Moulick, O. Zitka, L. Trnkova, V. Adam and R. Kizek, *Int. J. Electrochem. Sci.*, 2014, **9**, 3386-3397.
49. O. Zitka, M. Kominkova, S. Skalickova, H. Skutkova, I. Provaznik, T. Eckschlager, M. Stiborova, V. Adam, L. Trnkova and R. Kizek, *Int. J. Electrochem. Sci.*, 2012, **7**, 10544-10561.
50. N. O. Karpinich, M. Tafani, R. J. Rothman, M. A. Russo and J. L. Farber, *J. Biol. Chem.*, 2002, **277**, 16547-16552.

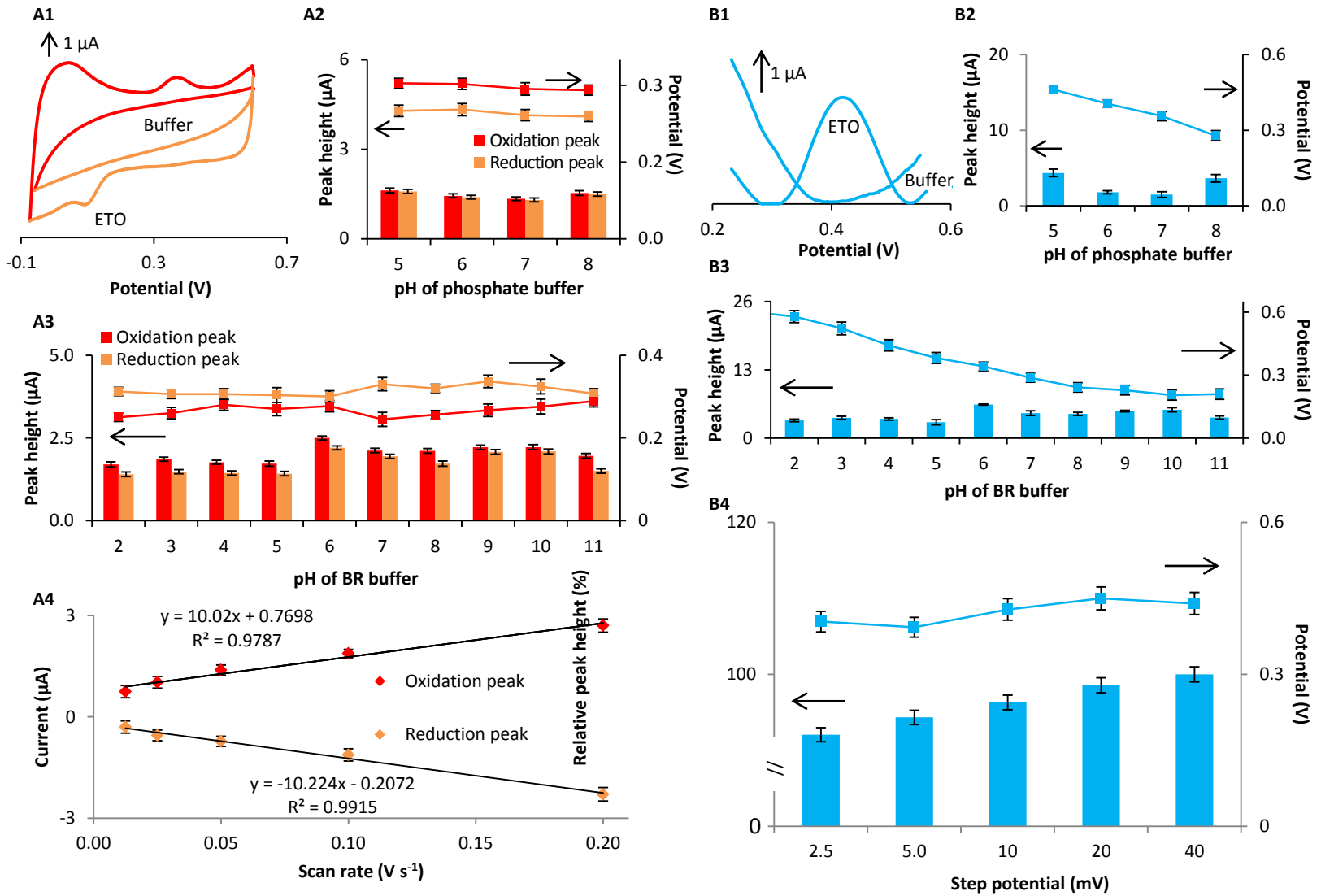

Figure 1

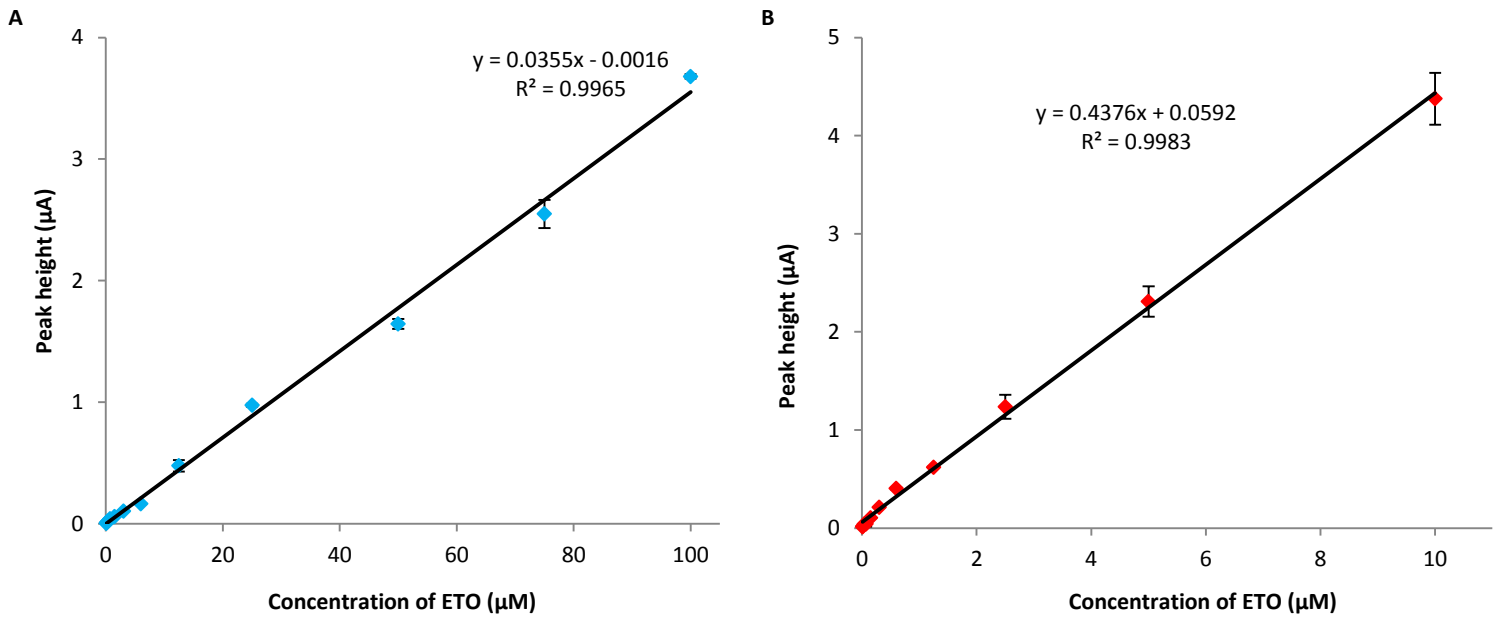

Figure 2

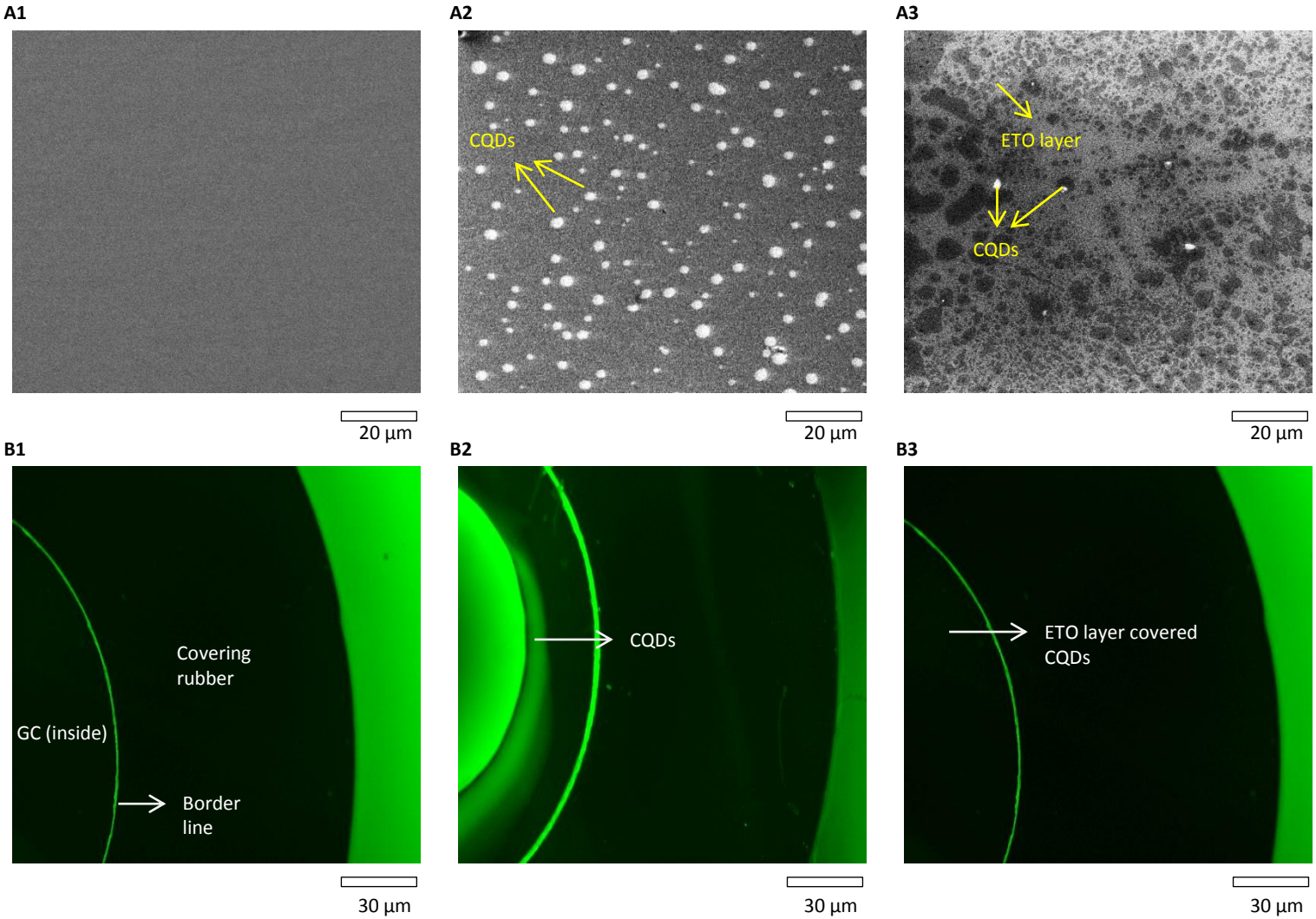

Figure 3

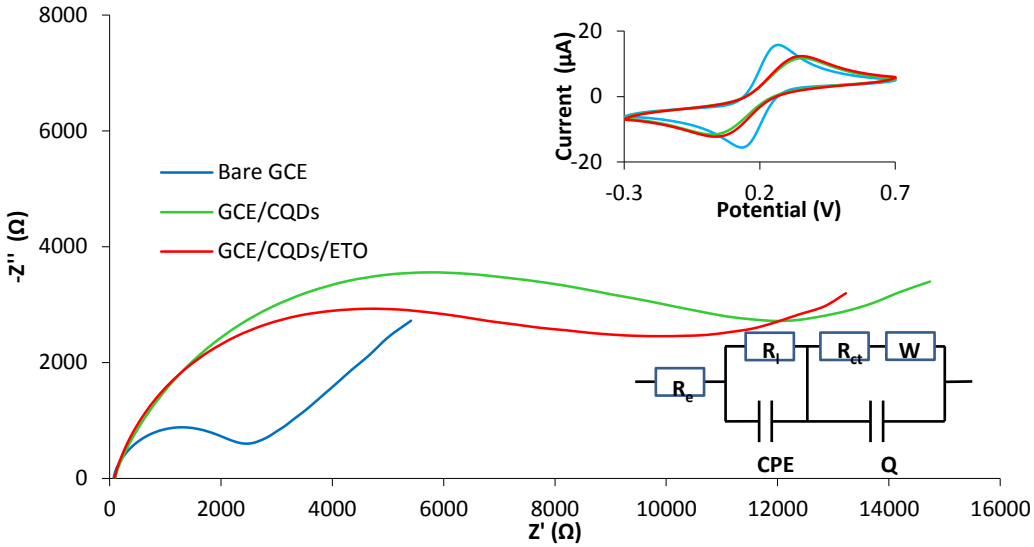

Figure 4

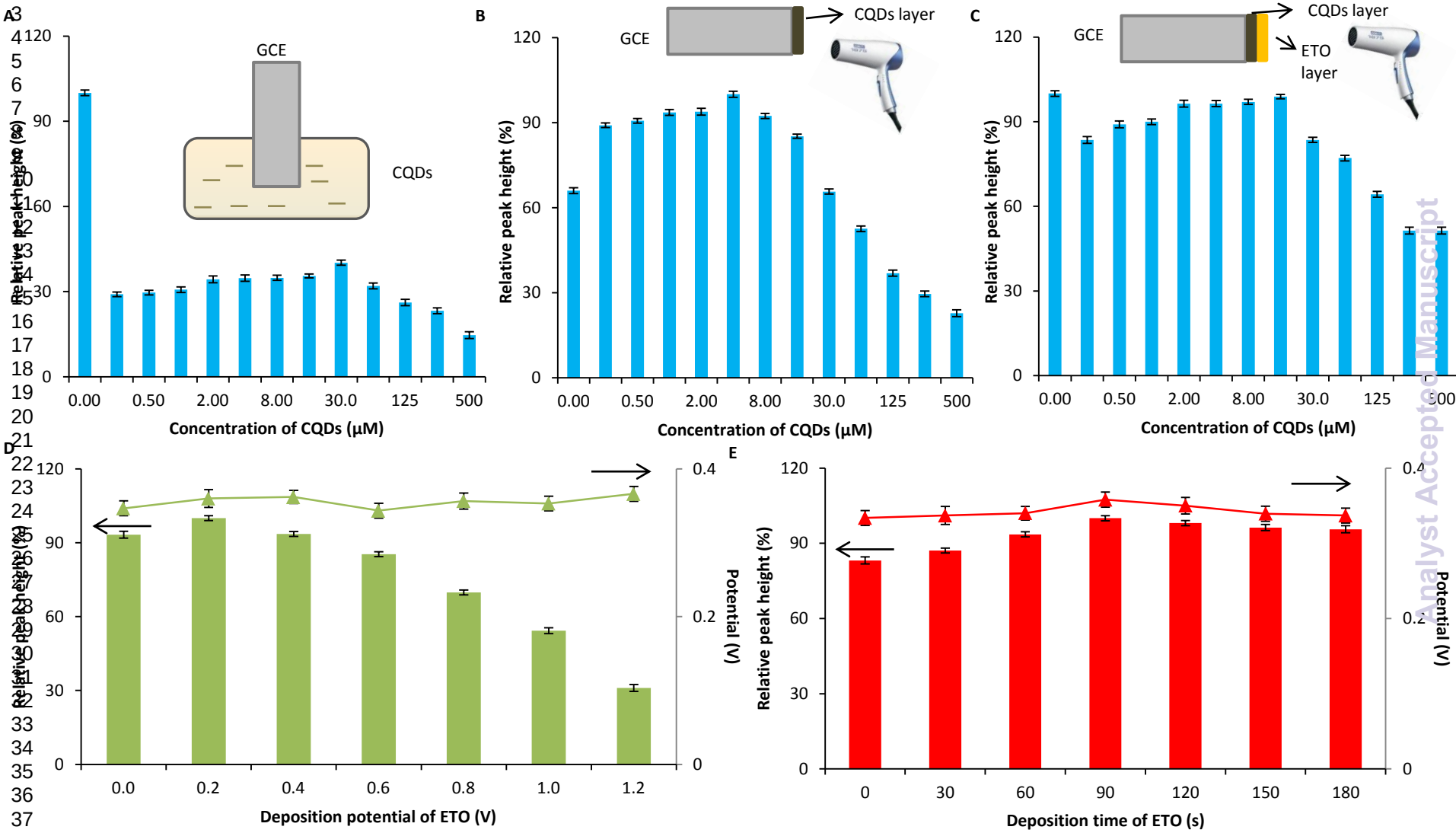

Figure 5

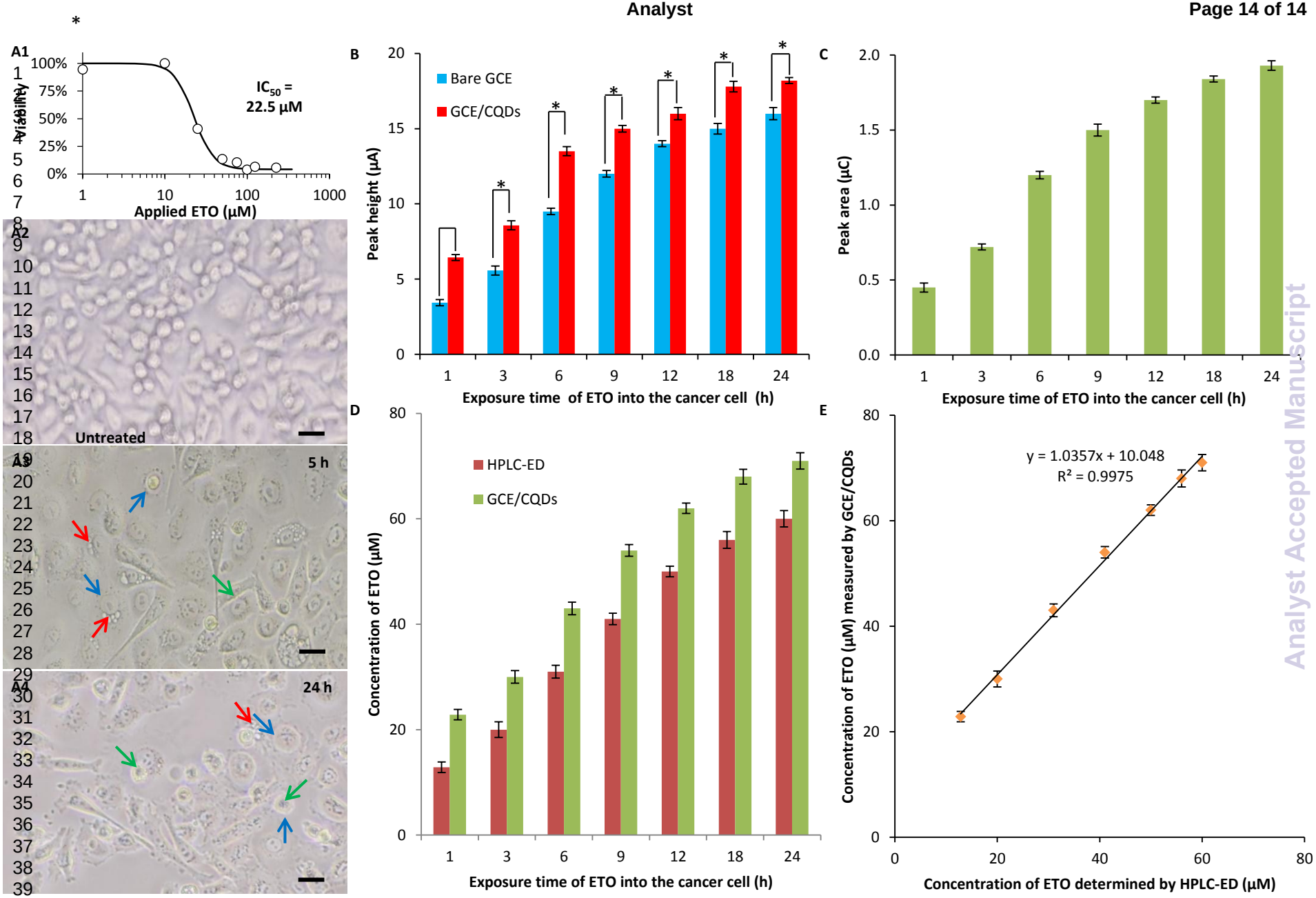

Figure 6